Notch3 marks clonogenic mammary luminal progenitor cells in vivo

Daniel Lafkas,[1,2,3,4] Veronica Rodilla,[1,2,3] Mathilde Huyghe,[1,2,3] Larissa Mourao,[1,2,3] Hippokratis Kiaris,[4] and Silvia Fre[1,2,3]

[1]Institut Curie, Centre de Recherche, 75248 Paris, Cedex 05, France
[2]Centre National de la Recherche Scientifique, Unité Mixte de Recherche 3215, 75248 Paris, Cedex 05, France
[3]Institut National de la Santé et de la Recherche Medicale U934, 75248 Paris, Cedex 05, France
[4]Department of Biological Chemistry, University of Athens Medical School, Athens 11527, Greece

The identity of mammary stem and progenitor cells remains poorly understood, mainly as a result of the lack of robust markers. The Notch signaling pathway has been implicated in mammary gland development as well as in tumorigenesis in this tissue. Elevated expression of the Notch3 receptor has been correlated to the highly aggressive "triple negative" human breast cancer. However, the specific cells expressing this Notch paralogue in the mammary gland remain unknown. Using a conditionally inducible Notch3-CreERT2^{SAT} transgenic mouse, we genetically marked Notch3-expressing cells throughout mammary gland development and followed their lineage in vivo. We demonstrate that Notch3 is expressed in a highly clonogenic and transiently quiescent luminal progenitor population that gives rise to a ductal lineage. These cells are capable of surviving multiple successive pregnancies, suggesting a capacity to self-renew. Our results also uncover a role for the Notch3 receptor in restricting the proliferation and consequent clonal expansion of these cells.

Introduction

Mammary epithelial cells form a network of branching ducts composed of a luminal and a basal myoepithelial layer. Luminal cells are subdivided into ductal cells, which line the mammary lumen, and alveolar cells, which give rise to alveolar units at pregnancy. The mammary gland shows remarkable plasticity, giving rise to a milk-producing organ at pregnancy (Oakes et al., 2006), which reverts to a virginlike state by responding to specific apoptotic signals during involution, when milk production is no longer needed (Watson, 2006). Central to this morphogenetic cycle are thought to be mammary stem cells (Williams and Daniel, 1983; Smith and Chepko, 2001), initially suggested to reside in the basal layer of the mammary duct (Shackleton et al., 2006; Stingl et al., 2006). More recent studies afforded new insights into the morphogenesis of the mammary epithelium, revealing hierarchical cell lineage relationships. A subset of luminal cells with specific regenerative capacity were recently uncovered (Sleeman et al., 2007; Regan et al., 2012; Shehata et al., 2012; Šale et al., 2013), and elegant in vivo lineage-tracing experiments confirmed the existence of two distinct adult stem cell populations in the mouse mammary gland, one for each compartment of the ductal bilayer, which give rise only to their respective compartment of origin (Van Keymeulen et al., 2011).

Breast cancer is the most common tumor in women, and the vast majority of breast tumors, particularly the poorly differentiated ones, are thought to arise from luminal progenitors (Prat and Perou, 2009; Molyneux et al., 2010). Thus, elucidating the lineage hierarchies that contribute to the development of the mammary gland is not only essential in understanding the morphogenesis of the gland but also in gaining insights into the cellular origins of mammary tumors, knowledge that may have therapeutic implications. Yet, the high cellular heterogeneity of the mammary epithelium and, most importantly, the lack of robust markers, have made the analyses of lineages quite challenging.

Notch pathway activity is known to be associated with stem cells in many tissues, such that it has been successfully used to trace lineages in the intestine and, more recently, in the mammary gland (Fre et al., 2011; Šale et al., 2013). This pathway controls cell differentiation and proliferation decisions

Correspondence to Silvia Fre: silvia.fre@curie.fr

Abbreviations used in this paper: 4-OHT, 4-hydroxytamoxifen; APC, Allophycocyanin; ER-α, estrogen receptor α; PR, progesterone receptor; qRT-PCR, quantitative RT-PCR; TEB, terminal end bud.

Supplemental material can be found at:
http://doi.org/10.1083/jcb.201307046

The Rockefeller University Press $30.00
J. Cell Biol. Vol. 203 No. 1 47–56
www.jcb.org/cgi/doi/10.1083/jcb.201307046

throughout development and adult homeostasis, by linking the fate of one cell to that of its neighbors. Cell-to-cell communication is achieved through the interaction of the Notch receptor expressed on one cell with membrane-bound ligands expressed on adjacent cells. All four Notch receptor paralogues, Notch1, 2, 3, and 4, have been shown to be expressed in the developing mammary gland (Bouras et al., 2008; Raouf et al., 2008; Raafat et al., 2011). Given the association of Notch with stem and progenitor cell populations, the expression of each paralogue may be used as a lineage marker. We have thus generated new transgenic mice that allowed us to use an in vivo lineage tracing approach to follow Notch-related cell lineages (Fre et al., 2011; Šale et al., 2013). We recently reported the tracing of Notch2 lineages in the mammary gland uncovering two hitherto unidentified epithelial lineages, revising significantly our understanding of mammary morphogenesis.

In this study, we focused on Notch3, a receptor that has been recently associated with the highly aggressive "triple negative" breast cancer (Yamaguchi et al., 2008; Turner et al., 2010; Speiser et al., 2013) and, of relevance for the present study, was found to be involved in the maintenance of stem cell quiescence in several tissues (Kuang et al., 2007; Kitamoto and Hanaoka, 2010; Kent et al., 2011; Mourikis et al., 2012; Alunni et al., 2013). Our analysis reveals that Notch3 is expressed in highly clonogenic luminal progenitor cells that are mostly found in a nonproliferative state but can get activated during mammary gland development to produce luminal daughter cells that can survive multiple cycles of pregnancy and involution. Our results using gain-of-function Notch3 mutant mice suggest that the proliferation of these cells is controlled by Notch3 activity.

Results and discussion

Notch3 is expressed in a subset of luminal cells

To conditionally label Notch3-expressing cells in vivo, we relied on our reporter strain Notch3-CreERT2^{SAT} in which a CreERT2 cassette is knocked in into the first exon of the *Notch3* locus (Fre et al., 2011). To follow cell lineages, we crossed them to a double-fluorescent reporter line, R26^{mTmG} (Muzumdar et al., 2007). In Notch3-CreERT2^{SAT}/R26^{mTmG} mice, membrane-bound GFP (mG) marks cells in which Cre-mediated recombination has occurred after hydroxytamoxifen induction (4-hydroxytamoxifen [4-OHT]). Notch3-CreERT2^{SAT}/R26^{mTmG} bigenic mice were injected with a single dose of 4-OHT (1 mg/20 g of body weight) at different developmental stages. The analysis of mice 24 h after Cre induction allowed us to detect the cells that express the Notch3 receptor but not their progeny. Even though the CreERT2 system is intrinsically mosaic, preventing us to target all Notch3-expressing cells, the clear enrichment in Notch3 expression we found in GFP$^+$-sorted cells (Fig. S1 B) indicates that these cells represent a subpopulation of mammary luminal cells that expresses the Notch3 receptor. At this time point, we detected histologically rare marked cells along the mammary ducts, representing 0.4 ± 0.03% of the total luminal compartment (Fig. S1 A). All of the Notch3-expressing cells at all developmental stages are marked by the luminal marker CK8 (cytokeratin 8) and do not express basal CK5 (cytokeratin 5; Fig. 1, A–J), confirming and extending previous expression studies (Bouras et al., 2008; Raafat et al., 2011). In addition, we observed that GFP-labeled cells consistently show strong nuclear levels of the polycomb group transcriptional repressor Bmi1 (Fig. S1, C and D), commonly associated with uncommitted progenitor cells in diverse tissues (Lessard and Sauvageau, 2003; Molofsky et al., 2003; Park et al., 2003).

The expression of membrane-tethered GFP in the R26^{mTmG} reporter mouse allows visualization of cellular protrusions otherwise indistinguishable from neighboring cells. By confocal microscopy, we observed that several GFP$^+$ cells extended long cellular protrusions that crossed the myoepithelial layer and came in close proximity with the basement membrane (Fig. S1, E and F). Similar protrusions have been previously described and suggested to be a characteristic of progenitor cells (Smith and Chepko, 2001; Oakes et al., 2006). Given that the ligands for Notch receptors appear to be differentially localized between the stroma and the myoepithelial layer of the mammary gland (Xu et al., 2012), it is conceivable that these protrusions may serve the purpose of achieving selective receptor activation and signaling by providing access to local cues from the microenvironment.

Notch3-expressing cells give rise to a luminal lineage

To further characterize the Notch3-expessing luminal cells in vivo, we induced Notch3-CreERT2^{SAT}/R26^{mTmG} mice with a single dose of 4-OHT at different developmental stages and followed their lineages at distinct time points after induction (Fig. S2). Regardless of the developmental stage of the mice at induction, Notch3-labeled cells invariably give rise to clusters of luminal cells. When mice were induced before puberty, at 3 wk of age, only single GFP$^+$ luminal cells could be detected 24 h after 4-OHT administration (Fig. 1, A and B; and Fig. 2 A). 3 wk after this prepubertal induction, the labeled cells expanded, generating small clones of GFP$^+$ cells (Fig. 2 B). An additional chase of 3 wk to adulthood (6-wk chase) resulted in further expansion of these clones (Fig. 2 C). The same type of clonal expansion was observed when mice were induced during puberty, at 6 wk of age (unpublished data). Induction of adult mice, after completion of mammary gland development, followed by a chase of 3 mo without going through pregnancy, also generated clusters of GFP$^+$ luminal progeny (Fig. 2 D). Thus, Notch3-expressing cells persist for a long time, eventually giving rise to luminal lineages during adult homeostasis. Of note, the GFP$^+$ progeny of single Notch3-expressing cells is heterogeneous for the expression of progesterone receptor (PR; Fig. 2, E and F) and estrogen receptor α (ER-α; Fig. 2, G and H), indicating that one cell can give rise to different lineages within the same clone. The analysis of the expression of these hormone receptors 24 h after induction shows that GFP$^+$ cells are also heterogeneous in their expression of ER-α and PR (Fig. S3). To examine whether all GFP-labeled cells have progenitor properties, we quantified the rate of their clonal expansion during puberty. Mice were induced at four weeks of age and were analyzed every week ($n = 3$ mice per time point) until the age of 8 wk (Fig. S2). This analysis revealed that 70% of Notch3-expressing luminal cells expand and give rise to clones, but 30% remain as single cells over the course of pubertal

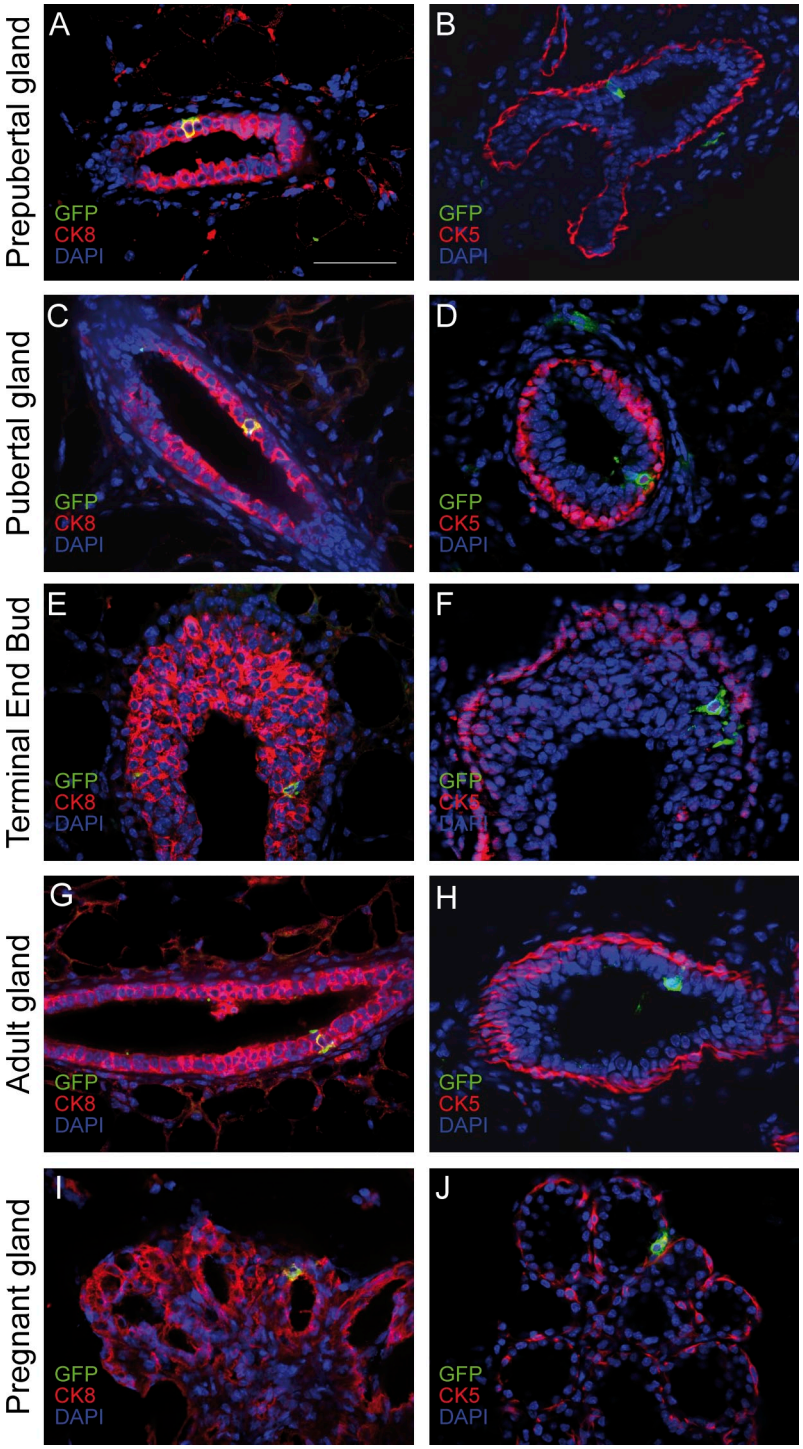

Figure 1. **Notch3 is specifically expressed in luminal cells at all developmental stages.** (A–J) Notch3-CreERT2^{SAT}/R26^{mTmG} mice were induced with 4-OHT at different developmental stages and analyzed 24 h later. Notch3-expressing cells (marked in green) are labeled by the luminal marker CK8 and not by the myoepithelial marker CK5. Representative sections of ducts from prepubertal mice (3 wk of age; A and B), pubertal mice (6 wk of age; C–F), adult mice (9 wk of age; G and H), and pregnant mice (I and J). Bar, 50 µm.

development, which lasts 4 wk (Fig. 2 I and Table S1). Conversely, the quantification of clonal expansion of CK8-expressing luminal cells, in the same developmental window, indicated that only 40% of luminal cells give rise to clones, as previously shown (Van Keymeulen et al., 2011). This important difference supports the notion that, unlike the ubiquitous luminal marker CK8, Notch3-CreERT2^{SAT} mice may target a specific luminal cell subpopulation with progenitor properties.

When we analyzed Notch3 lineages during pregnancy, we found that they contributed to the formation of alveolar buds, independent of the age of induction (Fig. 2 J). However, both GFP-positive and -negative luminal cells are found in alveoli, reflecting the polyclonal origin of these structures. To further examine whether Notch3-expressing cells were able to persist during mammary gland remodeling in vivo, we analyzed mice that had undergone three successive pregnancies, lactations, and involutions and found that Notch3-derived luminal lineages survived cell death during involution, suggesting that they derived from single GFP^{+} progenitors capable of self-renewal (Fig. 2, K and L).

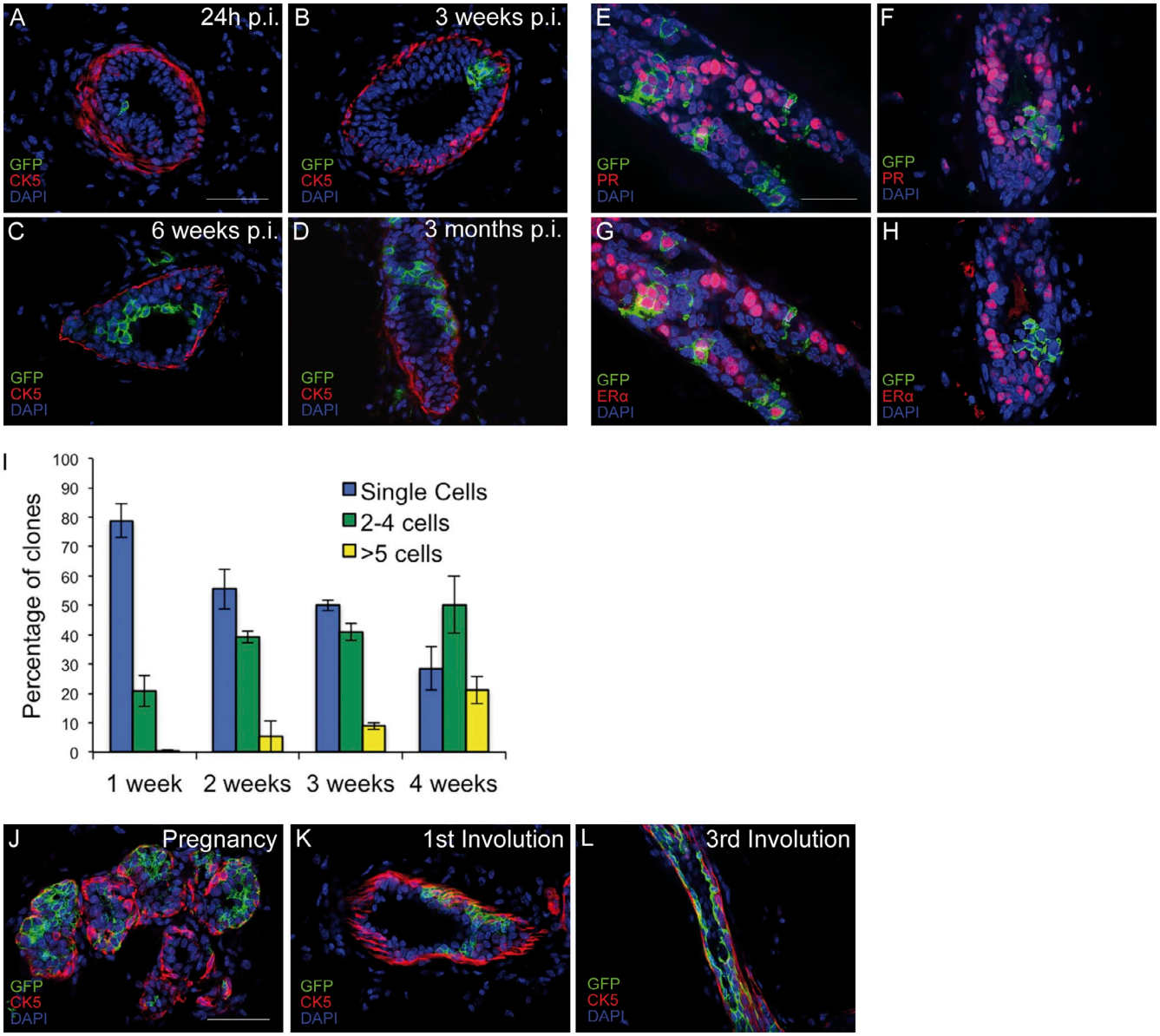

Figure 2. **Notch3-expressing cells give rise to luminal lineages.** Notch3-CreERT2^{SAT}/R26^{mTmG} mice were induced with a single dose of 4-OHT at different developmental stages, and the derived lineages were analyzed at different time points after induction. The basal layer is marked by CK5 staining in A–D and J–L, and nuclei are stained with DAPI. (A–C) Sections of glands of mice induced at 3 wk of age and analyzed after the following times: 24 h (A), 3 wk (B), and 6 wk (C). p.i., postinjection. D shows sections of glands from mice induced with 4-OHT as adults (9 wk of age) and analyzed after 3 mo. (E–H) GFP$^+$ progeny of Notch3-expressing cells contained cells that were both positive and negative for the progesterone receptor (PR; E and F) and the estrogen receptor α (ER-α; G and H). (I) Quantification of the rate of expansion of GFP$^+$ cells during puberty (4–8 wk of age). Mean (±SD) percentage of clones over the total number of clones counted per sample. Single cells, small clones of two to four cells, and large clones of more than five cells were counted. (J–L) Representative sections of mammary ducts from midpregnant mice induced at 3 wk of age (J), 4 wk after involution from mice induced at 6 wk of age after one pregnancy cycle (K), and after three consecutive pregnancies (L). Bars: (A–D and J–L) 50 µm; (E–H) 30 µm.

Notch3 expression defines cells with increased clonogenic potential

To investigate the clonogenic capacity of Notch3-expressing cells, we isolated by FACS GFP$^+$ cells from 6-wk-old females, after a 24-h induction with 4-OHT (Fig. S1 A), and seeded them on a feeder layer of irradiated fibroblasts. When we compared their in vitro colony-forming potential to that of GFP$^-$ luminal cells, we observed that GFP$^+$ cells formed clones with a 25% higher frequency (Fig. 3 A). To further characterize the GFP-marked cells, we tested whether they express CD49b (α-integrin), a recently established luminal progenitor marker (Shehata et al., 2012). After the protocol of Shehata et al. (2012), we subdivided the luminal compartment in three cell populations, based on their expression of CD49b and Sca1 (CD49b$^-$/Sca1$^+$, Cd49b$^+$/Sca1$^+$, and CD49b$^+$/Sca1$^-$). The distribution of GFP$^+$ cells in different luminal fractions using these two markers did not correlate Notch3 expression with a specific luminal subset (Fig. 3 B). Accordingly, quantitative RT-PCR (qRT-PCR) showed Notch3 expression in all three luminal subpopulations (Fig. 3 C). We then probed the colony-forming capacity of

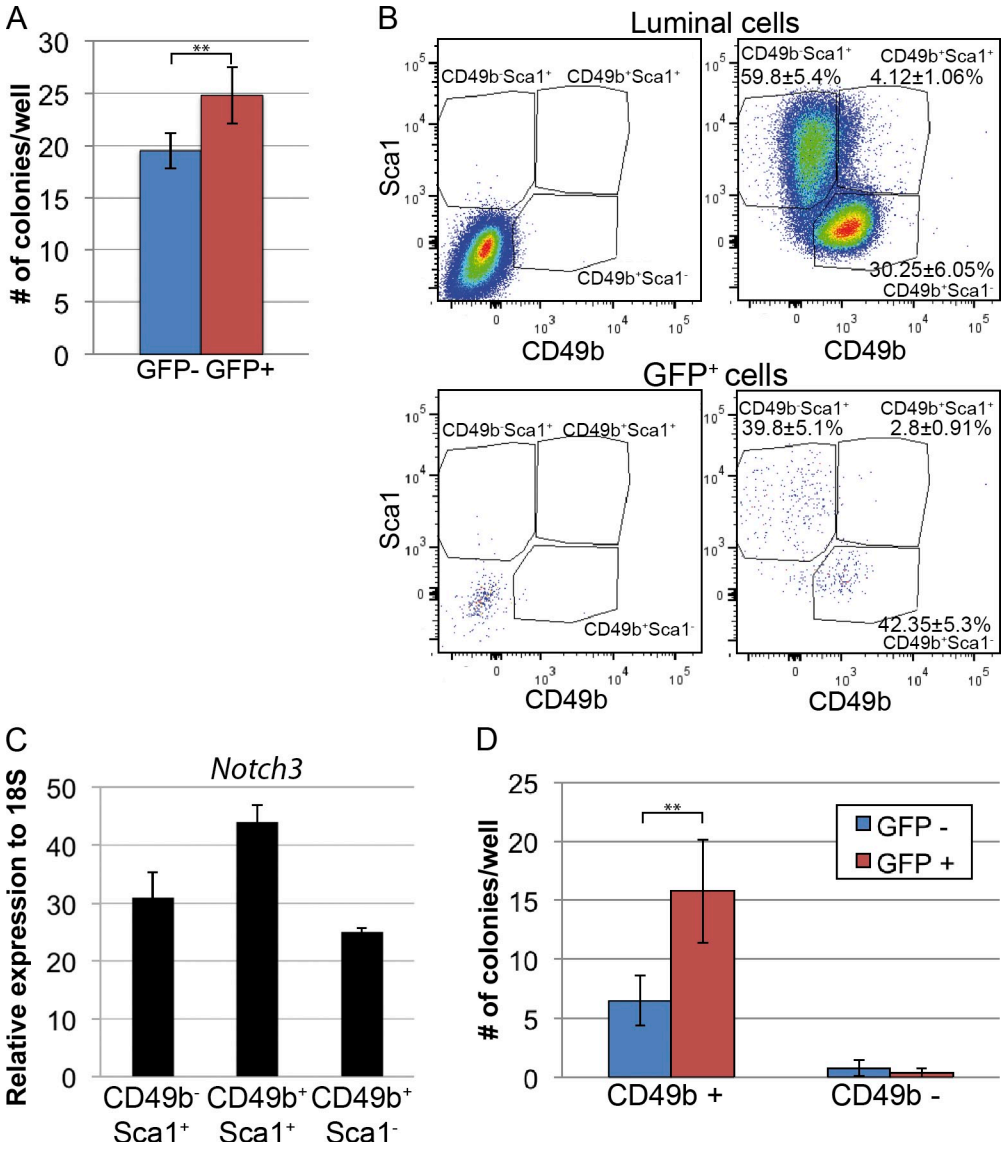

Figure 3. **Notch3-expressing cells present a high clonogenic potential.** (A) Number of colonies/well (±SD) formed by GFP$^+$ and GFP$^-$ luminal cells. (B) Distribution of GFP$^+$ cells (bottom plots) from 6-wk-old Notch3-CreERT2^{SAT}/R26^{mTmG} mice 24 h after induction (n = 3) among the three luminal subpopulations resolved by Sca1 and CD49b expression (top plots). The two left graphs represent controls without antibodies. The lines on the FACS plots correspond to the gates chosen to select the indicated cell populations: CD49b$^-$/Sca1$^+$, CD49b$^+$/Sca1$^+$, and CD49b$^+$/Sca1$^-$. (C) qRT-PCR showing the relative Notch3 RNA expression in Sca1$^+$/CD49b$^-$, Sca1$^+$/CD49b$^+$, and Sca1$^-$/CD49b$^+$ luminal fractions. Error bars represent the SDs of at least three independent experiments. (D) Number of colonies/well (±SD) formed by GFP$^+$ and GFP$^-$ cells in clonogenic (CD49b$^+$) and nonclonogenic (CD49b$^-$) luminal cell subpopulations. *, P ≤ 0.05; **, P ≤ 0.005. The p-values were calculated using the Student's t test.

CD49b$^+$ and CD49b$^-$ luminal cells and found that GFP$^+$ cells within the clonogenic CD49b$^+$ population had a 75% increased cloning efficiency compared with CD49b$^+$/GFP$^-$ luminal cells (Fig. 3 D). We confirmed that CD49b$^-$/Sca1$^+$ cells are nonclonogenic in this assay (Fig. 3 D, CD49b$^-$), as previously reported (Shehata et al., 2012). On the basis of this analysis, we propose that Notch3 is expressed in luminal progenitor cells with high clonogenic potential.

Notch3 luminal progenitor cells are transiently quiescent

To determine the proportion of Notch3-expressing cells that are actively cycling, we asked what percentage of GFP$^+$ cells is marked by the proliferation marker Ki67. Surprisingly, the vast majority of Notch3-expressing cells were negative for Ki67 at different developmental stages (prepuberty [Fig. 4 A], puberty [Fig. 4 B], and adulthood [Fig. 4 C]). The quantification of cycling GFP$^+$ cells at puberty showed that 98% of them were Ki67 negative (Fig. 4, A–D and G). The difference with total luminal cells was more prominent when we quantified Ki67 expression of GFP-labeled cells within the terminal end buds (TEBs; Fig. 4, D and H), where normally ∼50% of total luminal cells are proliferative. On the other hand, when we examined GFP-marked clones derived from Notch3-expressing cells 3 and 6 wk after induction at puberty, ∼12 and 20%, respectively, of these cells expressed Ki67 (Fig. 4, E–G), indicating that Notch3-expressing cells are not terminally differentiated but get activated asynchronously to proliferate and produce the observed clonal expansion of GFP$^+$ cells over time (Fig. 2 I).

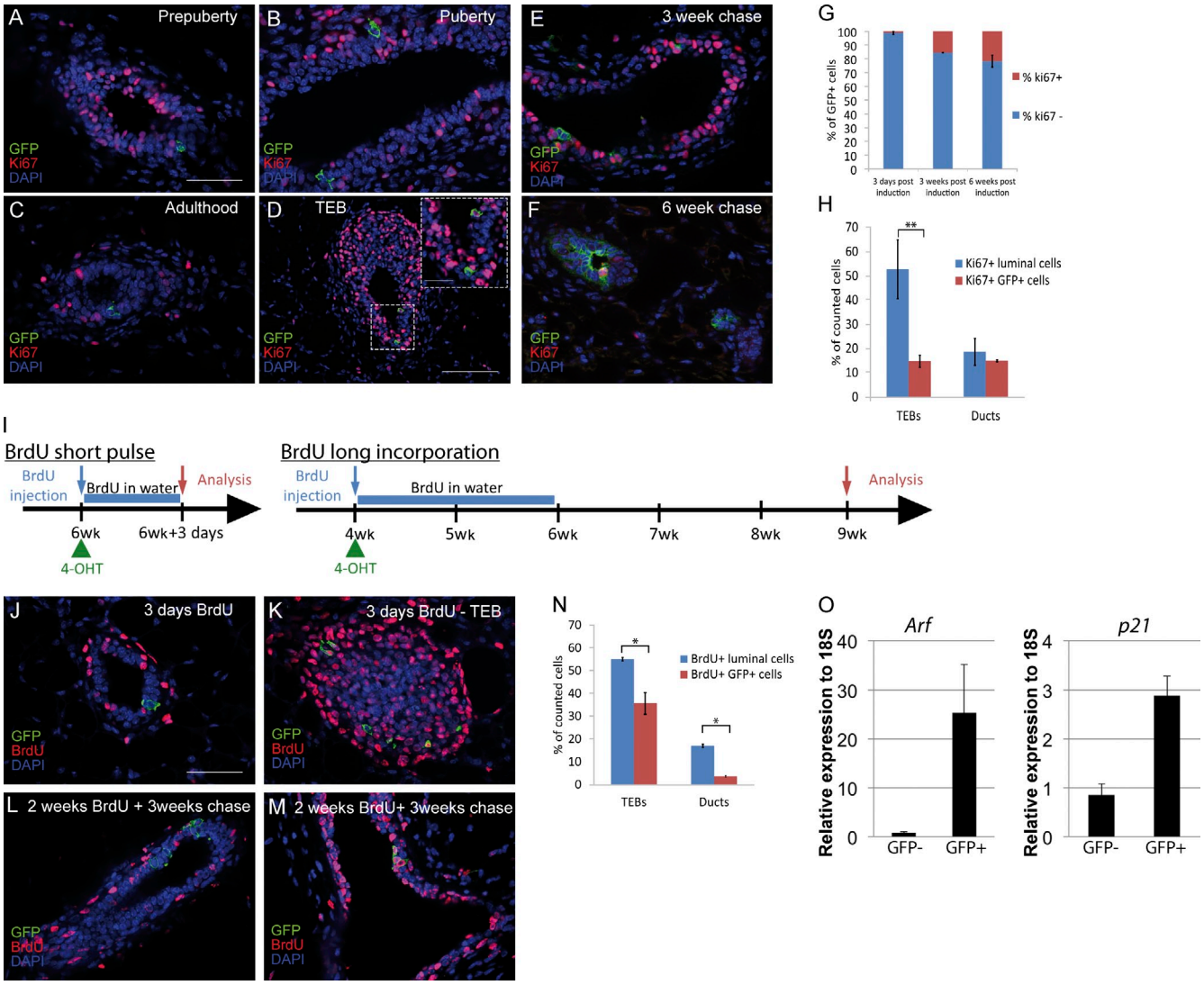

Figure 4. **GFP-expressing cells are mostly nonproliferative.** (A–D) Notch3-CreERT2^{SAT}/R26^{mTmG} mice induced with 4-OHT at the indicated developmental stages (n = 3 for each developmental stage) and analyzed 24 h later for their expression of the proliferation marker Ki67. Single Notch3$^+$ cells (in green) are not labeled by Ki67, with few exceptions in the terminal end buds (TEB; in D). The inset in D is a magnification of the area delineated by a dashed box. (E and F) Mice induced at 3 wk of age and immunostained with Ki67 after a 3-wk (E) or a 6-wk (F) chase present marked lineages that contain Ki67$^+$ cells. (G) Mean (±SD) percentage of GFP$^+$ cells stained for Ki67 over the total number of GFP$^+$ cells counted. 98% of GFP$^+$ cells are negative for Ki67 3 d after induction (A–D and G). (H) Quantification of the percentage of Ki67$^+$ luminal cells in TEBs and ducts (n = 3). The percentage of Ki67$^+$/GFP$^+$ cells 24 h after induction is shown compared with the percentage of Ki67$^+$ cells within the total luminal population. (I) Schematic representation of the BrdU incorporation experiments for both the short pulse and the long incorporation experiments. (J and K) Immunostaining with anti-BrdU antibodies shows that most GFP-expressing cells are negative for BrdU after a short pulse of BrdU (J), again with few exceptions in the TEBs (K). The progeny of Notch3-epressing cells (in green in L and M) contains both BrdU$^-$ (L) and BrdU$^+$ (M) clones after a long incorporation of BrdU. (N) Quantification of the percentage of BrdU$^+$ total luminal or GFP$^+$ cells in TEBs and ducts after a short BrdU pulse shows a striking reduction in the number of cycling GFP$^+$ cells, as it is the case for Ki67 (H). (O) Relative expression to the 18S housekeeping gene of Ink4/Arf and p21/Waf1 in GFP$^-$ and GFP$^+$ luminal cells indicates elevated expression of cell cycle inhibitors in GFP$^+$ cells. (N and O) Error bars represent the SDs of at least three independent experiments. *, P ≤ 0.05; **, P ≤ 0.005. The p-values were calculated using the Student's t test. Bars: (A–C, E, F, and J–M) 40 µm; (D, main image) 100 µm; (D, inset) 25 µm.

To better define the apparent quiescent state of Notch3-expressing cells, we analyzed their capacity to incorporate BrdU. Pubertal Notch3-CreERT2^{SAT}/R26^{mTmG} mice were injected with 4-OHT and with 50 µg/ml BrdU on day 0. Mice were then kept on continuous BrdU feeding for either a consecutive 3 d and sacrificed immediately after (short pulse; Fig. 4, I–K) or for 2 wk and sacrificed 3 wk thereafter (long incorporation; Fig. 4, I , L, and M). Although the majority of GFP$^+$ cells was negative for BrdU (98% in ducts and 65% in TEBs) after the short BrdU pulse (Fig. 4, J, K, and N), both BrdU-negative (Fig. 4 L) and BrdU-positive (Fig. 4 M) clones were observed after the long incorporation chase, further indicating that these cells are not terminally differentiated and that they can enter the cell cycle asynchronously. Importantly, GFP$^+$ cells show elevated expression levels of the cell cycle inhibitors p21/WAF1 and Ink4/Arf compared with GFP$^-$ luminal cells (Fig. 4 O), further corroborating their nonproliferative state. Our results reveal that Notch3 gene expression marks, in vivo, a luminal progenitor cell population that is maintained in a transiently non-proliferative state but can reenter the cell cycle, responding to yet unknown cues, to expand and give rise to luminal daughter cells.

Notch3 activation restricts the expansion of luminal progenitors

Based on these observations, we were prompted to ask whether a functional correlation exists between levels of Notch3 activity and the proliferative state of GFP-labeled cells. To examine this, we expressed a constitutively active Notch3 receptor in Notch3-expressing cells and their progeny, by crossing Notch3-CreERT2^{SAT}/R26^{mTmG} mice to a gain-of-function mouse line, in which the intracellular form of Notch3 (N3IC) is conditionally inserted into the ROSA26 locus (R26-N3IC^{SAT}; Fig. 5 A). We then quantified the clonal expansion in triple transgenic mice Notch3-CreERT2^{SAT}/R26^{mTmG}/R26-N3IC^{SAT} after a 4-wk chase. We found that in mice expressing N3IC, the number of clones generated was reduced by almost 50% compared with the clones generated in control Notch3-CreERT2^{SAT}/R26^{mTmG} mice (Fig. 5 B and Table S1). The reduced ability of these cells to generate marked progeny paralleled an increase in the number of single cells found 4 wk after induction (Fig. 5 B, blue histogram). No overt phenotype was observed, probably because Notch3-CreERT2^{SAT} mice target very few cells (0.1% of mammary epithelial cells). Expression of the N3IC transgene was evident both by the presence of the floxed allele in genomic DNA extracts in the presence of 4-OHT (Fig. 5 C, lanes 3 and 5) and by the elevated expression of intracellular Notch3 without significant changes in extracellular Notch3 levels, as detected by qRT-PCR using appropriate oligonucleotides (oligos; Fig. 5 D). Importantly, we observed that N3IC-expressing cells show increased expression of the cell cycle inhibitors Ink4/Arf and the cyclin-dependent kinase inhibitor p21/Waf1 (Fig. 5 E), which are also strongly expressed in cells targeted by Notch3-CreERT2^{SAT} (Fig. 4 O), further confirming their nonproliferative state. These results are consistent with the notion that sustained Notch3 activation can keep luminal cells in a transiently quiescent state. Consequently, we propose that luminal progenitors need to down-regulate Notch3 signaling to ensure luminal lineage expansion, as illustrated in the model depicted in Fig. 5 F. In this context, it is worth considering that previous studies in the muscle and in cell cultures suggested a functional role for Notch3 signaling and Hes1, a canonical Notch target gene, in maintaining cellular quiescence (Kuang et al., 2007; Sang and Coller, 2009; Kitamoto and Hanaoka, 2010; Kent et al., 2011; Mourikis et al., 2012; Alunni et al., 2013).

The role of Notch signals in oncogenesis has often been attributed to their positive influence on cell proliferation (Kiaris et al., 2004; Fre et al., 2009; Artavanis-Tsakonas and Muskavitch, 2010). Such a role presents an apparent contradiction with the results we obtained in this study because Notch3 activity seems to keep cells in a nonproliferative, resting state in the normal mammary gland. However, it is conceivable that in pathological conditions, Notch3 may contribute to increased survival of a cellular population, by protecting it against drugs that target highly proliferative cells.

Materials and methods

Mice

The generation of Notch3-CreERT2^{SAT} knockin mice has been previously described (Fre et al., 2011). The targeting vector included a genomic fragment covering the promoter region, exon1, and exon2 of the *Notch3* locus. Exon1, between the translation start site and the end of exon1, was replaced with a cassette containing the CreERT2 ORF, a polyadenylation signal and a flippase recognition target–flanked neomycin resistance gene. This results in expression of tamoxifen-inducible CreERT2 recombinase in all cells in which the promoter of Notch3 is active. These mice were crossed to a double-fluorescent reporter mouse strain R26^{mTmG} (Muzumdar et al., 2007), which was obtained from Jackson ImmunoResearch Laboratories, Inc. To generate R26-N3IC^{SAT} mice, the mouse the N3IC cDNA (amino acids 1,668–2,318) was amplified by PCR, sequenced, and cloned directly into a ROSA26 targeting vector. This targeting construct included a lox-STOP-lox cassette at the 5′ end of the N3IC sequence and a polyadenylation sequence at the 3′ end. This construct was electroporated into embryonic stem cells (C57BL/5NTac). All experiments and procedures involving animals were in strict accordance with the French and European legislations for the Protection of Vertebrate Animals used for Experimental and other Scientific Purposes and were approved by the Departmental Direction of Populations Protection (approval number: B75-05-18). Husbandry and supply of animals as well as maintenance and care of the animals in exempt of pathogen species environments before and during experiments fully satisfies the animal's needs and welfare. Suffering of the animals has been kept to a minimum: no procedures inflicting pain have been performed.

Transgenic mouse genotyping

Mice were genotyped by PCR using the following primers: Notch3-CreERT2^{SAT} 1228_23, 5′-ATAGGAACTTCAAAATGTCGCG-3′, and 1239_22, 5′-CCCAGCTGCTGCATCTCTGC-3′ (187 bp); Notch3 wild type 1239_21, 5′-TCGTCGCCTGATGGCCTTGC-3′, and 1239_22, 5′-CCCAGCTGCTGCATCTCTGC-3′ (244 bp); R26-N3IC^{SAT} 1336_5, 5′-GCATGGTGGAAGAGCTCATC-3′, and 1336_6, 5′-GTCCAAGTGATCTGTGATCTCC-3′ (257 bp); ROSA26 wild type 1260_1, 5′-GAGACTCTGGCTACTCATCC-3′, and 1260_2, 5′-CCTTCAGCAAGAGCTGGGGAC-3′ (585 bp); R26^{mTmG} Rosa1, 5′-AAAGTCGCTCTGAGTTGTTAT-3′; Pcag-r105, 5′-GTCGTTGGGCGGTCAG-3′ (250 bp); and N3IC floxed forward, 5′-CCTCCTGGCTTCTGAGGAC-3′, reverse (unfloxed), 5′-CTCGTCCTGCAGTTCATTCA-3′ (504 bp), and reverse (floxed), 5′-ACCTCCCCCATCAGACTCTC-3′ (432 bp).

Conditional labeling of Notch3 lineages

Notch3-CreERT2^{SAT}/R26^{mTmG} and control Notch3-CreERT2^{SAT} females ranging from 3 to 9 wk of age were induced with a single i.p. injection of 4-OHT (1 mg/20 g mouse body weight; H7904; Sigma-Aldrich). For expression analysis, animals were sacrificed 24 h after induction. For lineage-tracing experiments, animals were sacrificed at different time points ranging from 48 h to several months after induction. For each time point, four mammary glands of at least three mice were analyzed. No GFP expression was observed in noninduced transgenic mice.

Histology and immunofluorescence labeling

Freshly dissected mammary glands from Notch3-CreERT2^{SAT}/R26^{mTmG} females were fixed at room temperature with 4% PFA in PBS for 2 h and either embedded in optimal cutting temperature medium (VWR International) or embedded in paraffin. Samples were sectioned at 10 or 20 µm. For immunofluorescence staining, frozen sections were permeabilized with 0.2% Triton X-100–PBS for 45 min and blocked for 1 h with 5% FBS and 2% BSA. The following primary antibodies were used: chicken anti-GFP (1:1,000; ab13970; Abcam), rabbit anti-CK5 (1:1,000; PRB-160P; Covance), rabbit anti-PR (1:300; sc-7208; Santa Cruz Biotechnology, Inc.), and rabbit anti-Ki67 (1:300; ab15580; Abcam). Paraffin-embedded sections were rehydrated through a gradient of ethanol. Subsequently, antigen retrieval was achieved by boiling in 10 mM citrate buffer (20 min) for all antibodies. Staining was performed as mentioned previously for frozen sections. The following primary antibodies were used: mouse anti-CK8 (1:200; MMS-162P; Covance), mouse anti–ER-α (1:300; M7047; Dako), mouse anti-BrdU (1:200; 347580; BD), mouse anti–BMI-1 (1:100; 39993; Active Motif), mouse anti–α-smooth muscle actin (1:500; A2547; Sigma-Aldrich), and rabbit anti–Collagen type IV (1:80; AB756P; EMD Millipore). Secondary antibodies were incubated in blocking buffer for 1–2 h at room temperature. The following secondary antibodies were used: anti–chicken Alexa Fluor 488 (1:1,000; A-11039; Invitrogen), anti–rabbit Alexa Fluor 633 (1:1,000; A-21071; Invitrogen), anti–mouse Alexa Fluor 633 (1:1,000; A-21202; Invitrogen), and goat anti–mouse Cy3 (1:500; 115–165-003; Beckman Coulter). Nuclei were stained with DAPI. Analysis and counting of positively stained cells were performed on at least two sections for each of three different parts of at least two mammary glands per animal.

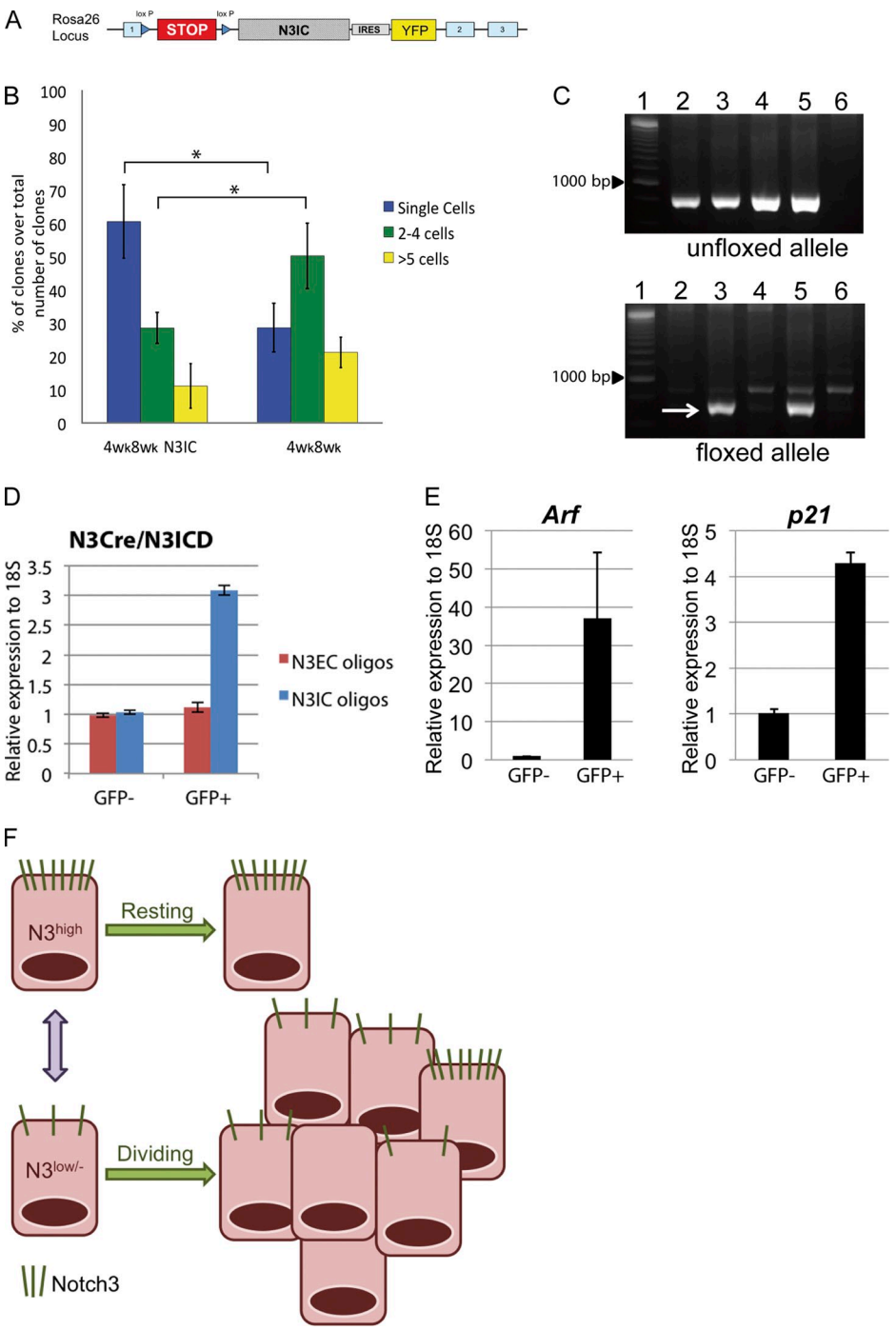

Figure 5. **Notch3 activation retains cells in a nonproliferative state.** (A) Schematic diagram of the N3IC targeting vector used for the generation of R26-N3IC^{SAT} knockin mice. The intracellular domain of the Notch3 receptor (N3IC) was knocked in to the ROSA26 locus followed by an internal ribosome entry site and a YFP gene. A lox-STOP-lox cassette blocks the expression of the transgene in the absence of Cre recombinase. (B) Quantification of clonal expansion upon constitutive Notch3 activation. Mean (±SD) percentage of clones (single cells, two to four cell clones, and clones bigger than five cells) over the total number of clones counted from Notch3-CreERT2^{SAT}/R26^{mTmG}/R26-N3IC^{SAT} mice (4wk8wk N3IC) compared with Notch3-CreERT2^{SAT}/R26^{mTmG} mice (4wk8wk). Mice were induced with a single dose of 4-OHT at 4 wk of age and analyzed at 8 wk of age. *, $P \leq 0.05$. The p-values were calculated using the Student's *t* test. (C) Genomic DNA PCR showing the unfloxed N3IC transgene (top) and the floxed N3IC allele (bottom, indicated by a white arrow). The floxed allele is amplified only upon 4-OHT induction. Lanes: (1) 1-kb molecular weight marker; (2) N3IC mouse1 no 4-OHT; (3) N3IC mouse1 + 4-OHT; (4) N3IC mouse2 no 4-OHT; (5) N3IC mouse2 + 4-OHT; and (6) nontransgenic control mouse. (D) qRT-PCR with specific oligos recognizing the extracellular (N3EC) or intracellular (N3IC) domain of Notch3 indicates sustained N3IC expression in GFP$^+$ cells sorted from Notch3-CreERT2^{SAT}/R26^{mTmG}/R26-N3IC^{SAT} mice 4 wk after induction. Note that the levels of endogenous Notch3 (detected with the N3EC oligos) are unchanged between GFP$^+$ and GFP$^-$ cells because the analysis has been performed on the progeny of Notch3-expressing cells 4 wk after induction, containing both Notch3$^+$ and Notch3$^-$ cells. (E) qRT-PCR analysis of sorted GFP$^-$ and GFP$^+$ cells from Notch3-CreERT2^{SAT}/R26^{mTmG}/R26N3IC^{SAT} mice 4 wk after induction shows elevated expression levels of Arf and p21 in N3IC-expressing GFP$^+$ cells. (D and E) Error bars represent the SD of at least three independent experiments. (F) Proposed model for the observed behavior of GFP-labeled cells. A luminal cell expressing high levels of Notch3 receptor (N3^{high}) is kept in a resting nonproliferative state until it down-regulates Notch3 expression (N3$^{low/-}$), allowing it to enter the cell cycle and give rise to a luminal lineage. The assumption is that only cells expressing high levels of Notch3 (N3^{high}) will be marked by Cre recombination, whereas proliferative N3$^{low/-}$ cells will not be labeled by GFP in this system.

Clonal expansion quantification

To quantify the clonal expansion on Notch3-expressing cells, we developed a protocol to remove the stroma surrounding the mammary gland by enzymatic digestion and visualize the remaining intact mammary ducts through compiled confocal z stacks. Freshly dissected mammary glands were incubated rocking in digestion medium containing 1,200 U/ml collagenase and 400 U/ml hyaluronidase for 2 h at 37°C. Tubes were centrifuged at 1,500 rpm for 3 min. The resuspended pellet was fixed for 20 min in 3 ml of 4% PFA in PBS at 4°C, in a 15-ml tube previously coated with FBS for 2 h. The fixed tissue was washed three times in PBS by pulse centrifuging at 1,500 rpm to remove single cells and muscle tissue. The tissue was then imaged on a confocal microscope on a cell culture dish (Fluorodish; World Precision Instruments). At least three mice per time point were analyzed and counted.

BrdU incorporation

BrdU (Sigma-Aldrich) was resuspended in PBS at a concentration of 5 mg/ml. Mice were injected with 50 mg BrdU/kg of body weight. BrdU was added to the drinking water at a concentration of 1 mg/ml supplemented with 2.5% wt/vol sucrose. For the short pulse, 5-wk-old mice were induced with 1 mg/20 g 4-OHT and injected with BrdU at day 0. BrdU was added to the drinking water, and mice were analyzed 3 d later. For the long incorporation, 5-wk-old mice were induced with 1 mg/20 g 4-OHT and injected with BrdU at day 0. BrdU was added to the drinking water and renewed every 2 d for 2 wk, after which mice were chased for 3 wk in normal drinking water. In each case, four mammary glands from two mice were analyzed.

Mammary cell preparation and flow cytometry

Bigenic Notch3-CreERT2^{SAT}/R26^{mTmG} females were induced with 4-OHT at 6 wk of age and sacrificed after 48 h. Single-cell suspensions from mammary glands were prepared essentially as previously described (Shackleton et al., 2006). Mammary glands were dissected from 6-wk-old female mice and mechanically dissociated with a scalpel and razor blade. The tissue was placed in culture medium (DMEM/F12 1:1 with L-glutamine supplemented with 500 ng/ml hydrocortisone, 10 ng/ml EGF, 5 µg/ml insulin, and 20 ng/ml cholera toxin) with 600 U/ml collagenase (Sigma-Aldrich) and 200 U/ml hyaluronidase (Sigma-Aldrich) and incubated for 1 h at 37°C. The resulting suspension was then treated with 0.25% trypsin-EDTA for 2 min and quenched with an equal volume of culture medium containing 10% FBS, 5 mg/ml dispase (Roche), and 0.1 mg/ml DNase (Sigma-Aldrich) for 3 min and then with 0.64% NH_4Cl for 3 min and finally filtrated through a 40-µm mesh. Dissociated cells were then incubated with antibodies in PBS (Ca/Mg^{2+} free), 1% BSA, 5 mM EDTA, 25 mM Hepes, pH 7.0, and 10 U/ml DNase for 20 min at a density of 40×10^6 cells/ml in the dark and on ice. The following antibodies were used: CD45-Allophycocyanin (APC) at 1:60 (clone 30-F11; BioLegend), CD31-APC at 1:60 (clone MEC13.3; BioLegend), Ter-119-APC at 1:60 (clone TER-119; BioLegend), CD24-phycoerythrin/Cy7 (Cyanin7) at 1:60 (clone M1/69; BioLegend), CD29–Alexa Fluor 700 at 1:60 (clone HMβ1-1; BioLegend), Sca-1–PerCP/Cy 5.5 at 1:60 (clone D7; BioLegend), and CD49b-phycoerythrin at 1:60 (clone HM-α; BioLegend). Debris and doublets were excluded by sequential gating on forward scatter area versus side scatter area followed by side scatter width versus side scatter area. DAPI and CD45, CD31, and ER-119 (Lin) staining was used to exclude nonviable cells, immune cells, endothelial cells, and erythrocytes, respectively. Cell analysis was performed on a FACS flow cytometer (LSR II; BD), and cell sorting was performed on a FACSAria (BD). Data were analyzed with the FlowJo software (TreeStar, Inc.).

Colony-forming assay

FACS-sorted single mammary epithelial cells were seeded on a feeder layer of irradiated NIH-3T3 fibroblasts. Fibroblasts were grown in DMEM medium (Invitrogen) supplemented with 10% FBS (Invitrogen) and 1% vol/vol penicillin/streptomycin (Invitrogen). The day before the experiment, fibroblasts were irradiated at 20 Gray and, after 3 h in culture, were seeded in 24-well plates at a density of 5,000 cells per well. Isolated epithelial cells were seeded on the feeder layer at a density of 300 cells/well and grown in DMEM/F12 1:1 (Invitrogen) supplemented with 10% FBS, 1% vol/vol penicillin/streptomycin (Invitrogen), 5 µg/ml insulin (Sigma-Aldrich), 10 ng/ml EGF (Sigma-Aldrich), and 10 ng/ml cholera toxin (Sigma-Aldrich). The growth of colonies was monitored daily, and the experiment was stopped after 6 d in culture. Colonies were stained with hematoxylin and counted. The experiment was repeated three times counting ≥12 wells per condition.

DNA and RNA extraction

DNA was extracted using the DNeasy Blood & Tissue kit (QIAGEN) according to the manufacturer's instructions. RNA was extracted from FACS-sorted cells using the RNeasy Mini kit (QIAGEN).

qRT-PCR

Reverse transcription (Superscript III; Invitrogen) was used for cDNA synthesis. The primers used for RT-PCR analyses were Arf forward, 5′-CGCAGGTTC-TTGGTCACTGTGAGG-3′, and reverse, 5′-TGCCCATCATCATCACCT-GGTCC-3′; p21 forward, 5′-TATTTAAGCCCCTCCCAACC-3′, and reverse, 5′-AGCTGGCCTTAGAGGTGACA-3′; N3EC forward, 5′-TTGTCTGGATG-GAAGCCCATG-3′, and reverse, 5′-ACTGAACTCTGGCAAACGCCT-3′; and N3IC forward, 5′-TGAACAACGTGGAGGCTACC-3′, and reverse, 5′-GCAGCCTGTCCAAGTGATCT-3′. qRT-PCR was performed in ViiA 7 by Life Technologies obtained from Applied Biosystems, using SYBR Green I Master kit (Roche).

Microscope image acquisition

Stained sections were mounted in imaging medium (Aqua-Poly/Mount; Polysciences, Inc.) and imaged on an inverted confocal spinning disk (CSU-X1 [Yokogawa Corporation of America and Roper Scientific] mounted on an inverted microscope [Eclipse-Ti; Nikon]) equipped with a camera (CoolSNAP HQ2; Photometrics) and a 405-, a 491-, a 561-, and a 633-nm laser. Images were taken with objectives ranging from 20 to 100×, with a numerical aperture between 0.3 and 1.4, depending on the objective used. Raw images were acquired with the MetaMorph software (Molecular Devices) and analyzed using ImageJ (National Institutes of Health).

Online supplemental material

Fig. S1 shows the characterization of Notch3-expressing cells. Fig. S2 shows a schematic representation of the timeline of 4-OHT induction and analyses for lineage-tracing experiments, presented in Fig. 2. Fig. S3 shows ER-α/PR expression in GFP$^+$ cells 24 h after induction. Table S1 gives raw data of the number and percentage of clones counted for each experimental condition in triplicates, for the analysis of clonal expansion presented in Fig. 2 (wild-type mice) and in Fig. 5 (Notch3 gain-of-function mice). Online supplemental material is available at http://www.jcb.org/cgi/content/full/jcb.201307046/DC1.

We are extremely grateful to Prof. Spyros Artavanis-Tsakonas for generously sharing the Notch3-CreERT2^{SAT} mice with us, for his support, and his precious and critical scientific advice. The authors would like to acknowledge the Cell and Tissue Imaging Platform of the Genetics and Developmental Biology Department (UMR3215/U934) of Institut Curie for help with light microscopy. We are particularly grateful to S. Boissel, C. Daviaud, and M. Garcia for precious help in the maintenance and care of the transgenic animals and to the Flow Cytometry Platform of Institut Curie. We also wish to thank S. Sale, A.S. Kaanta, A. Louvi, and the lab of M. Glukhova for constructive discussions, scientific insights, and technical advice.

This research was in part supported by the Association pour la Recherche contre le Cancer to S. Fre and by Labex DEEP (Développement, Epigénèse, Epigénétique et Potentiel) 11-LBX-0044.

Submitted: 8 July 2013
Accepted: 10 September 2013

References

Alunni, A., M. Krecsmarik, A. Bosco, S. Galant, L. Pan, C.B. Moens, and L. Bally-Cuif. 2013. Notch3 signaling gates cell cycle entry and limits neural stem cell amplification in the adult pallium. *Development*. 140:3335–3347. http://dx.doi.org/10.1242/dev.095018

Artavanis-Tsakonas, S., and M.A. Muskavitch. 2010. Notch: the past, the present, and the future. *Curr. Top. Dev. Biol.* 92:1–29. http://dx.doi.org/10.1016/S0070-2153(10)92001-2

Bouras, T., B. Pal, F. Vaillant, G. Harburg, M.L. Asselin-Labat, S.R. Oakes, G.J. Lindeman, and J.E. Visvader. 2008. Notch signaling regulates mammary stem cell function and luminal cell-fate commitment. *Cell Stem Cell*. 3:429–441. http://dx.doi.org/10.1016/j.stem.2008.08.001

Fre, S., S.K. Pallavi, M. Huyghe, M. Laé, K.P. Janssen, S. Robine, S. Artavanis-Tsakonas, and D. Louvard. 2009. Notch and Wnt signals cooperatively control cell proliferation and tumorigenesis in the intestine. *Proc. Natl. Acad. Sci. USA*. 106:6309–6314. http://dx.doi.org/10.1073/pnas.0900427106

Fre, S., E. Hannezo, S. Sale, M. Huyghe, D. Lafkas, H. Kissel, A. Louvi, J. Greve, D. Louvard, and S. Artavanis-Tsakonas. 2011. Notch lineages and activity in intestinal stem cells determined by a new set of knock-in mice. *PLoS ONE*. 6:e25785. http://dx.doi.org/10.1371/journal.pone.0025785

Kent, S., J. Hutchinson, A. Balboni, A. Decastro, P. Cherukuri, and J. Direnzo. 2011. ΔNp63α promotes cellular quiescence via induction and activation of Notch3. *Cell Cycle*. 10:3111–3118. http://dx.doi.org/10.4161/cc.10.18.17300

Kiaris, H., K. Politi, L.M. Grimm, M. Szabolcs, P. Fisher, A. Efstratiadis, and S. Artavanis-Tsakonas. 2004. Modulation of notch signaling elicits signature tumors and inhibits hras1-induced oncogenesis in the mouse mammary epithelium. *Am. J. Pathol.* 165:695–705. http://dx.doi.org/10.1016/S0002-9440(10)63333-0

Kitamoto, T., and K. Hanaoka. 2010. Notch3 null mutation in mice causes muscle hyperplasia by repetitive muscle regeneration. *Stem Cells*. 28:2205–2216. http://dx.doi.org/10.1002/stem.547

Kuang, S., K. Kuroda, F. Le Grand, and M.A. Rudnicki. 2007. Asymmetric self-renewal and commitment of satellite stem cells in muscle. *Cell*. 129:999–1010. http://dx.doi.org/10.1016/j.cell.2007.03.044

Lessard, J., and G. Sauvageau. 2003. Bmi-1 determines the proliferative capacity of normal and leukaemic stem cells. *Nature*. 423:255–260. http://dx.doi.org/10.1038/nature01572

Molofsky, A.V., R. Pardal, T. Iwashita, I.K. Park, M.F. Clarke, and S.J. Morrison. 2003. Bmi-1 dependence distinguishes neural stem cell self-renewal from progenitor proliferation. *Nature*. 425:962–967. http://dx.doi.org/10.1038/nature02060

Molyneux, G., F.C. Geyer, F.A. Magnay, A. McCarthy, H. Kendrick, R. Natrajan, A. Mackay, A. Grigoriadis, A. Tutt, A. Ashworth, et al. 2010. BRCA1 basal-like breast cancers originate from luminal epithelial progenitors and not from basal stem cells. *Cell Stem Cell*. 7:403–417. http://dx.doi.org/10.1016/j.stem.2010.07.010

Mourikis, P., R. Sambasivan, D. Castel, P. Rocheteau, V. Bizzarro, and S. Tajbakhsh. 2012. A critical requirement for notch signaling in maintenance of the quiescent skeletal muscle stem cell state. *Stem Cells*. 30:243–252. http://dx.doi.org/10.1002/stem.775

Muzumdar, M.D., B. Tasic, K. Miyamichi, L. Li, and L. Luo. 2007. A global double-fluorescent Cre reporter mouse. *Genesis*. 45:593–605. http://dx.doi.org/10.1002/dvg.20335

Oakes, S.R., H.N. Hilton, and C.J. Ormandy. 2006. The alveolar switch: coordinating the proliferative cues and cell fate decisions that drive the formation of lobuloalveoli from ductal epithelium. *Breast Cancer Res.* 8:207. http://dx.doi.org/10.1186/bcr1411

Park, I.K., D. Qian, M. Kiel, M.W. Becker, M. Pihalja, I.L. Weissman, S.J. Morrison, and M.F. Clarke. 2003. Bmi-1 is required for maintenance of adult self-renewing haematopoietic stem cells. *Nature*. 423:302–305. http://dx.doi.org/10.1038/nature01587

Prat, A., and C.M. Perou. 2009. Mammary development meets cancer genomics. *Nat. Med.* 15:842–844. http://dx.doi.org/10.1038/nm0809-842

Raafat, A., A.S. Goldhar, M. Klauzinska, K. Xu, I. Amirjazil, D. McCurdy, K. Lashin, D. Salomon, B.K. Vonderhaar, S. Egan, and R. Callahan. 2011. Expression of Notch receptors, ligands, and target genes during development of the mouse mammary gland. *J. Cell. Physiol.* 226:1940–1952. http://dx.doi.org/10.1002/jcp.22526

Raouf, A., Y. Zhao, K. To, J. Stingl, A. Delaney, M. Barbara, N. Iscove, S. Jones, S. McKinney, J. Emerman, et al. 2008. Transcriptome analysis of the normal human mammary cell commitment and differentiation process. *Cell Stem Cell*. 3:109–118. http://dx.doi.org/10.1016/j.stem.2008.05.018

Regan, J.L., H. Kendrick, F.A. Magnay, V. Vafaizadeh, B. Groner, and M.J. Smalley. 2012. c-Kit is required for growth and survival of the cells of origin of Brca1-mutation-associated breast cancer. *Oncogene*. 31:869–883. http://dx.doi.org/10.1038/onc.2011.289

Šale, S., D. Lafkas, and S. Artavanis-Tsakonas. 2013. Notch2 genetic fate mapping reveals two previously unrecognized mammary epithelial lineages. *Nat. Cell Biol.* 15:451–460. http://dx.doi.org/10.1038/ncb2725

Sang, L., and H.A. Coller. 2009. Fear of commitment: Hes1 protects quiescent fibroblasts from irreversible cellular fates. *Cell Cycle*. 8:2161–2167. http://dx.doi.org/10.4161/cc.8.14.9104

Shackleton, M., F. Vaillant, K.J. Simpson, J. Stingl, G.K. Smyth, M.L. Asselin-Labat, L. Wu, G.J. Lindeman, and J.E. Visvader. 2006. Generation of a functional mammary gland from a single stem cell. *Nature*. 439:84–88. http://dx.doi.org/10.1038/nature04372

Shehata, M., A. Teschendorff, G. Sharp, N. Novcic, A. Russell, S. Avril, M. Prater, P. Eirew, C. Caldas, C.J. Watson, and J. Stingl. 2012. Phenotypic and functional characterization of the luminal cell hierarchy of the mammary gland. *Breast Cancer Res.* 14:R134. http://dx.doi.org/10.1186/bcr3334

Sleeman, K.E., H. Kendrick, D. Robertson, C.M. Isacke, A. Ashworth, and M.J. Smalley. 2007. Dissociation of estrogen receptor expression and in vivo stem cell activity in the mammary gland. *J. Cell Biol.* 176:19–26. http://dx.doi.org/10.1083/jcb.200604065

Smith, G.H., and G. Chepko. 2001. Mammary epithelial stem cells. *Microsc. Res. Tech.* 52:190–203. http://dx.doi.org/10.1002/1097-0029(20010115)52:2<190::AID-JEMT1005>3.0.CO;2-O

Speiser, J.J., C. Erşahin, and C. Osipo. 2013. The functional role of notch signaling in triple-negative breast cancer. *Vitam. Horm.* 93:277–306. http://dx.doi.org/10.1016/B978-0-12-416673-8.00013-7

Stingl, J., P. Eirew, I. Ricketson, M. Shackleton, F. Vaillant, D. Choi, H.I. Li, and C.J. Eaves. 2006. Purification and unique properties of mammary epithelial stem cells. *Nature*. 439:993–997.

Turner, N., M.B. Lambros, H.M. Horlings, A. Pearson, R. Sharpe, R. Natrajan, F.C. Geyer, M. van Kouwenhove, B. Kreike, A. Mackay, et al. 2010. Integrative molecular profiling of triple negative breast cancers identifies amplicon drivers and potential therapeutic targets. *Oncogene*. 29:2013–2023. http://dx.doi.org/10.1038/onc.2009.489

Van Keymeulen, A., A.S. Rocha, M. Ousset, B. Beck, G. Bouvencourt, J. Rock, N. Sharma, S. Dekoninck, and C. Blanpain. 2011. Distinct stem cells contribute to mammary gland development and maintenance. *Nature*. 479:189–193. http://dx.doi.org/10.1038/nature10573

Watson, C.J. 2006. Involution: apoptosis and tissue remodelling that convert the mammary gland from milk factory to a quiescent organ. *Breast Cancer Res.* 8:203. http://dx.doi.org/10.1186/bcr1401

Williams, J.M., and C.W. Daniel. 1983. Mammary ductal elongation: differentiation of myoepithelium and basal lamina during branching morphogenesis. *Dev. Biol.* 97:274–290. http://dx.doi.org/10.1016/0012-1606(83)90086-6

Xu, K., J. Usary, P.C. Kousis, A. Prat, D.Y. Wang, J.R. Adams, W. Wang, A.J. Loch, T. Deng, W. Zhao, et al. 2012. Lunatic fringe deficiency cooperates with the Met/Caveolin gene amplicon to induce basal-like breast cancer. *Cancer Cell*. 21:626–641. http://dx.doi.org/10.1016/j.ccr.2012.03.041

Yamaguchi, N., T. Oyama, E. Ito, H. Satoh, S. Azuma, M. Hayashi, K. Shimizu, R. Honma, Y. Yanagisawa, A. Nishikawa, et al. 2008. NOTCH3 signaling pathway plays crucial roles in the proliferation of ErbB2-negative human breast cancer cells. *Cancer Res.* 68:1881–1888. http://dx.doi.org/10.1158/0008-5472.CAN-07-1597